Programmable Materials (2023), **Vol. 1**:e10 1–15
doi:10.1017/pma.2023.9

PROGRAMMABLE MATERIALS

RESEARCH ARTICLE

Harnessing length and height changes in thermoresponsive programmable materials

Dilip Chalissery[1], Tobias Rümmler[1], Fabian Ziervogel[2], Chris Eberl[3] and Thorsten Pretsch[1]

[1]Fraunhofer Institute for Applied Polymer Research IAP, Potsdam, Germany.
[2]Fraunhofer Institute for Machine Tools and Forming Technology IWU, Dresden, Germany.
[3]Fraunhofer Institute for Mechanics of Materials IWM, Freiburg, Germany.

Corresponding author: Thorsten Pretsch; Email: thorsten.pretsch@iap.fraunhofer.de

Received: 29 March 2023; **Revised:** 8 June 2023; **Accepted:** 21 June 2023

Keywords: active smart structures; advanced functional materials; logical operations and functional dependencies; manufacturing processes for programmable materials; mechanisms providing programmability; shape-changing smart structures

Abstract

Shape-memory polymers can be used to develop thermoresponsive programmable materials that can take on sensory and actuator tasks as their ambient temperature changes. In this contribution, a self-synthesised poly(1,10-decylene adipate) diol-based polyester urethane (PEU) was used for their fabrication. After processing the PEU into filaments, programmable materials, including a gear-like object, the teeth of a 'bevel gear' and a unit cell, were additively manufactured by fused filament fabrication. In any case, a thermomechanical treatment was conducted that involved the deformation of the polymer at 75°C. After cooling to 15°C, the programmable materials were unloaded and the thermoresponsiveness between 23°C and 58°C was investigated. A maximum thermoreversible change in height of about 39% was detected for the 'gear'. With regard to the 'bevel gear', proof of feasibility was provided for use as overheating protection, so that a force transmission could be switched off when heated and switched on when cooled down. The unit cell actuated under a weak external load of 0.01 N, thus exhibiting thermoreversible length changes of about 45%.

Introduction

Shape-memory polymers (SMPs) are smart materials that are able to fix a temporary shape after a thermomechanical treatment, also denoted as 'programming'. When applying a suitable stimulus, SMPs are able to almost completely recover the initial shape. In other words, the so-called 'one-way (1W) shape-memory effect (SME)' is triggered (Liu et al., 2007; Dietsch and Tong, 2007; Ratna and Karger-Kocsis, 2008; Pretsch, 2010; Sun et al., 2012; Chalissery et al., 2019). Here, shape recovery is an entropically driven process based on entropy elasticity according to the theory of rubber elasticity (Holme, 1806). Among stimulus-responsive SMPs that have been investigated so far, thermoresponsive SMPs are the most widely investigated (Yin et al., 2006; Hoffman, 2013; Kim and Matsunaga, 2017). After triggering the 1W-SME, an SMP requires another thermomechanical treatment to become thermoresponsive again. By contrast, in the case of the so-called 'two-way (2W) SME', an SMP is able to switch between two temperature bistable states without the need for further programming (Chung et al., 2008; Bothe and Pretsch, 2012; Hager et al., 2015; Zhao et al., 2015; Zare et al., 2019; Scalet,

2020; Ke et al., 2020). For SMPs, the 2W-SME has been investigated on semicrystalline polymers since these materials fulfil the necessary morphological requirements (Westbrook et al., 2011; Zare et al., 2019). Here, the main driving forces for the 2W transition are the crystallisation of polymer chains and the melting of the associated crystallites, the same as entropy elasticity (Westbrook et al., 2011; Zhao et al., 2015; Schönfeld et al., 2021). In particular, phase-segregated thermoplastic polyurethanes (TPUs; Kim et al., 1996; Li et al., 1997; Lee et al., 2001; Ji et al., 2007; Huang et al., 2010; Müller and Pretsch, 2010; Pereira and Oréfice, 2010; Pretsch and Müller, 2010; Wang et al., 2010; Petchsuk et al., 2012; Bothe et al., 2013; Liu et al., 2016; Ren et al., 2016; Mirtschin and Pretsch, 2017), which are built up of hard and soft segments, have proven their potential over chemically cross-linked SMPs due to the capability of mechanical recycling. In the last decade, scientists have unveiled how to implement the 2W-SME into physically cross-linked TPUs (Bothe et al., 2013; Ke et al., 2020; Schönfeld et al., 2021). For instance, Schönfeld et al. (2021) developed a poly(1,10-decylene adipate) (PDA)-based polyester urethane (PEU) and processed it via the additive manufacturing technique fused filament fabrication (FFF). As a result, objects could be obtained that were programmed by tensile deformation at 75°C, cooling to 23°C while holding the elongated shape, followed by unloading. Adjacently, the printed object shrank on heating and expanded on cooling with a maximum thermoreversible strain of 16% (Schönfeld et al., 2021)). A few years earlier, Bothe and Pretsch (2012) applied substantial tensile deformation to achieve deformation-induced crystallisation in the soft segment phase of a commercially available PEU. Actuation was dependent on the underlying constant stress conditions. For instance, actuation of 35% occurred in the fifth measurement cycle at 1.5 MPa and of 19% in the 20th cycle at 1.25 MPa. Likewise, significant actuation was verified in other contributions on physically cross-linked PEUs (Behl et al., 2013; Fan et al., 2017, 2018a,b, 2020).

Despite the steadily growing number of publications on 2W SMPs in the last few years, the question arises to what extent actuation can be realised by more complex motion sequences or even by the parallel motion of several parts within a single component. The answer is the design and construction of programmable materials from SMPs and the implementation of the 2W-SME by thermomechanical treatment. Programmable materials are currently the subject of intensive research (Zhang et al., 2011; Restrepo et al., 2016; Berwind et al., 2018; Fischer et al., 2020; Jin et al., 2020; Walter et al., 2020; Schönfeld et al., 2021; Specht et al., 2021; Chalissery et al., 2022) and use mechanisms on molecular as well as mesoscopic levels to implement information processing. Here, material functionality meets structural design. Complex types of material behaviours can be realised by implementing conditional behaviour (e.g., IF. . .THEN. . .ELSE) or design functional dependencies (e.g., E, $\alpha = f(T)$). Furthermore, programmable materials can be designed to be independent of external power supplies by harvesting environmental changes, for example, temperature changes. Essentially, they can be implemented as self-sufficient materials with complex behaviour based on physical computing, similar to what can be found in nature. Thus, they entail an all-in-one sensor, actuator, controlling unit, and energy harvesting functionality (Zhang et al., 2011; Takeuchi et al., 2022). In this work, a thermoresponsive material is facilitated as a programmable temperature control for a gearbox. The idea is to provide an overheating protection; in other words, the force transmission in gear units is switched from ‘on’ to ‘off’ and vice versa as a result of heating and cooling, respectively. Taking a first step in this direction, the same PDA-based PEU, which was recently developed and characterised by promising actuation (Schönfeld et al., 2021), was selected as the base material. After developing a gear-like design and rapid prototyping via FFF, the object was thermomechanically treated and actuation was studied while systematically varying the temperature. Following a different design, but addressing the same application, the thermoresponsiveness of a ‘bevel gearbox’ containing 2W actuating elements was examined. With the same idea of transferring a programmable material into bistable temperature states, a third demonstrator was developed and its actuation behaviour was investigated. In this context, it will be shown that the design of the thermoresponsive programmable material leads to the realisation of a considerably larger change in length compared to the pure base material in linear form, which potentially will be able to switch on and off a load bearing structure (Chalissery, 2023).

https://doi.org/10.1017/pma.2023.9 Published online by Cambridge University Press

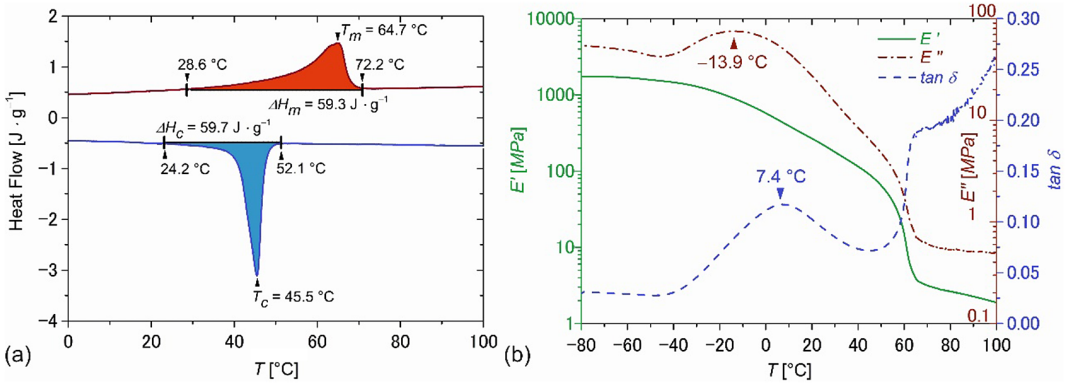

Figure 1. *Thermal and thermomechanical properties of PDA-based PEU as determined by DSC (a, second heating and cooling with temperature rates of 10°C·min^{-1}, the enthalpies of melting ΔH_m, red coloured area, and crystallisation ΔH_c, blue coloured area, are included) and DMA (b, the temperature dependence of storage modulus E', loss modulus E" and loss factor tan δ at a heating rate of 3°C·min^{-1}).*

Results

In this contribution, a PDA-based PEU, which was developed in our previous works (Schönfeld et al., 2021; Chalissery et al., 2022), was selected as the functional base material.

The thermal and thermomechanical properties of the PDA-based PEU were analysed (Figure 1) by means of differential scanning calorimetry (DSC, Figure 1a) and dynamic mechanical analysis (DMA, Figure 1b).

In the DSC measurement, a broad melting transition, ranging from 29°C to 72°C, with a peak located at 65°C and a crystallisation transition spreading from 52°C to 24°C with a peak at 46°C were detected (Figure 1a). The signals were assigned to the phase transitions of PDA, which served as the soft segment in the phase-segregated PEU. In the DMA measurement (Figure 1b), a similar evolution was detected for the storage modulus *E*' and for tan *δ* as in our previous works (Schönfeld et al., 2021; Chalissery et al., 2022). Again, *E*' exhibited a two-step decline as associated with the devitrification and melting of the PDA phase. At temperatures of about 65°C and thus above the melting transition of PDA, the hard segments of the PEU ensured that the polymer still had a sufficiently high degree of dimensional stability. The evolution of tan *δ* exhibited a broad signal at about 7°C, which was assigned to the glass transition temperature T_g (Schönfeld et al., 2021; Chalissery et al., 2022). The synthesised PEU was processed to filament, which was then used to manufacture demonstrators employing the FFF method.

Next, an object characterised by a gear-like design (Figure 2) was developed. The 'gear' was designed in such a way that a compressive load applied during thermomechanical treatment would shift the out-of-plane parts resulting in an entirely flat structure (Figure 2). Specifically, the 'gear' consisted of three inverted 'V'-shaped structures in each line (Figure 2b). The structures were designed to translate any vertical motion directly into horizontal motion. When the 'gear' was compressed from top to bottom, the 'V'-shaped structures bent to form a flat shape, increasing the outer diameter of the 'gear' (Figure 2b–g). This change could possibly establish contact with similarly designed objects in a kind of force transmission system. While the gear design obviously maximises the effect of radial change, it could be simple to improve the torque-bearing abilities by radial elements, which also need to expand with the radius. A more elaborate mechanical model will be designed in later iterations.

The next step was to develop a method for thermomechanical treatment, which later enabled almost stress-free actuation of the 'gear'. Here, an approach of compression bending was followed by means of a DMA device, which was also used to identify the ideal actuation conditions (Figure 3). It is noteworthy that this approach did not allow the characterisation of length changes with regard to

https://doi.org/10.1017/pma.2023.9 Published online by Cambridge University Press

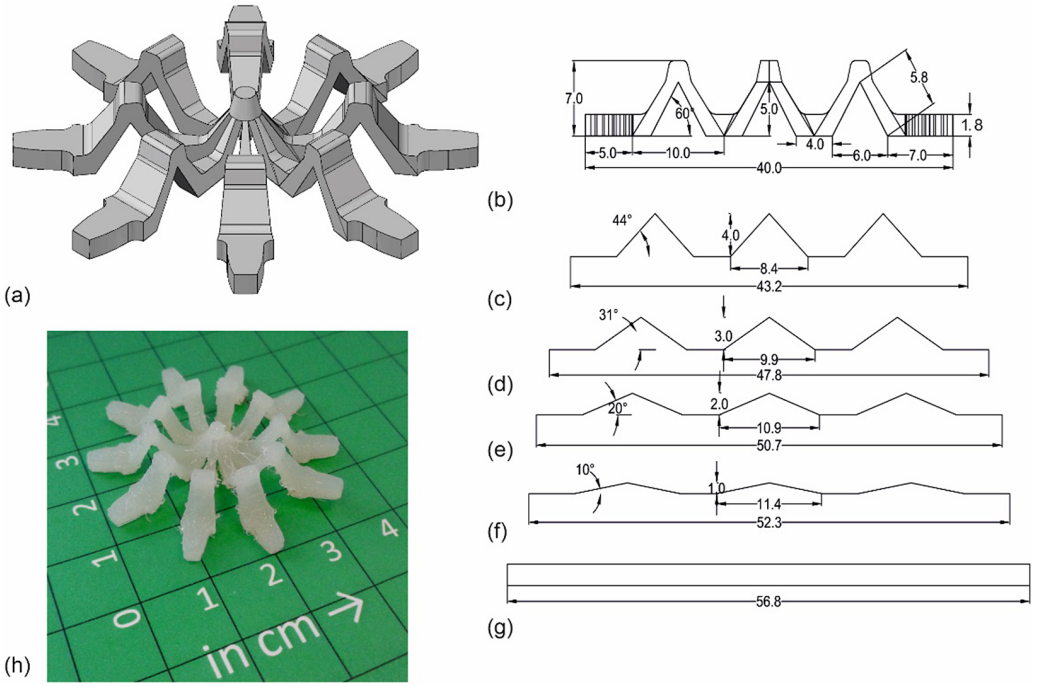

Figure 2. *Technical drawings and an additively manufactured demonstrator for a simplified programmable gear-like object in its (a) isometric view, (b) front view including the dimensions of the original shape, (c–g) the potential shape modifications due to stepwise loading with regard to individual displacements, and (h) after additive manufacturing via FFF. In panels (b–g), the dimensions are provided in millimetres.*

the diameter of the object. In detail, the thermomechanical treatment consisted of heating to 75°C, applying a compressive force of 17 N, ensuring that only compression bending and no pressure crushing occurred, cooling to 15°C, and holding the temperature constant for 30 min, followed by unloading to 0.01 N. In response to the applied compressive force, the height of the object was reduced from 7 mm to 1.8 mm, at which the latter corresponded to the thickness of the 'gear tooth'. Upon temperature cycling, thermoreversible changes in the height of the object and thus an actuation could be detected in every single measurement cycle, even when the upper temperature T_{max} was continuously increased from 55°C to 70°C, while the lower temperature was left at 15°C (Figure 3a). The driving mechanisms of actuation were mostly heating-induced melting of the PDA soft segment, leading to a movement out of the plane of the flat 'gear', corresponding to a raising of the object and thus an increase in its height h (Figure 3b), and cooling-induced crystallisation of the PDA soft segment, resulting in the movement back to the rather planar shape of the 'gear', along the direction of the compressive force applied during thermomechanical treatment, associated with a decrease in h.

Only a small quantity of crystallisable segments was present when selecting a lower maximum temperature T_{max}, because a larger part of the PDA phase was still in a crystalline state (Figure 1a), resulting in weak elongation on heating and weak contraction on cooling, as can be seen in Figure 3c, at which Δh describes the evolution of changes in the height of the object under a constant external load of 0.01 N. By contrast, the increase in T_{max} can be associated with an increase in the proportion of crystallisable segments, because more PDA crystals were molten (Figure 1a). When selecting a T_{max} of 58°C, the most pronounced actuation could be detected, characterised by a thermoreversible change in the height of 39% as averaged for the last two cycles, which can be seen in the associated diagram (Figure 3c). The respective schematic temperature bistable states of the object at 58°C and

https://doi.org/10.1017/pma.2023.9 Published online by Cambridge University Press

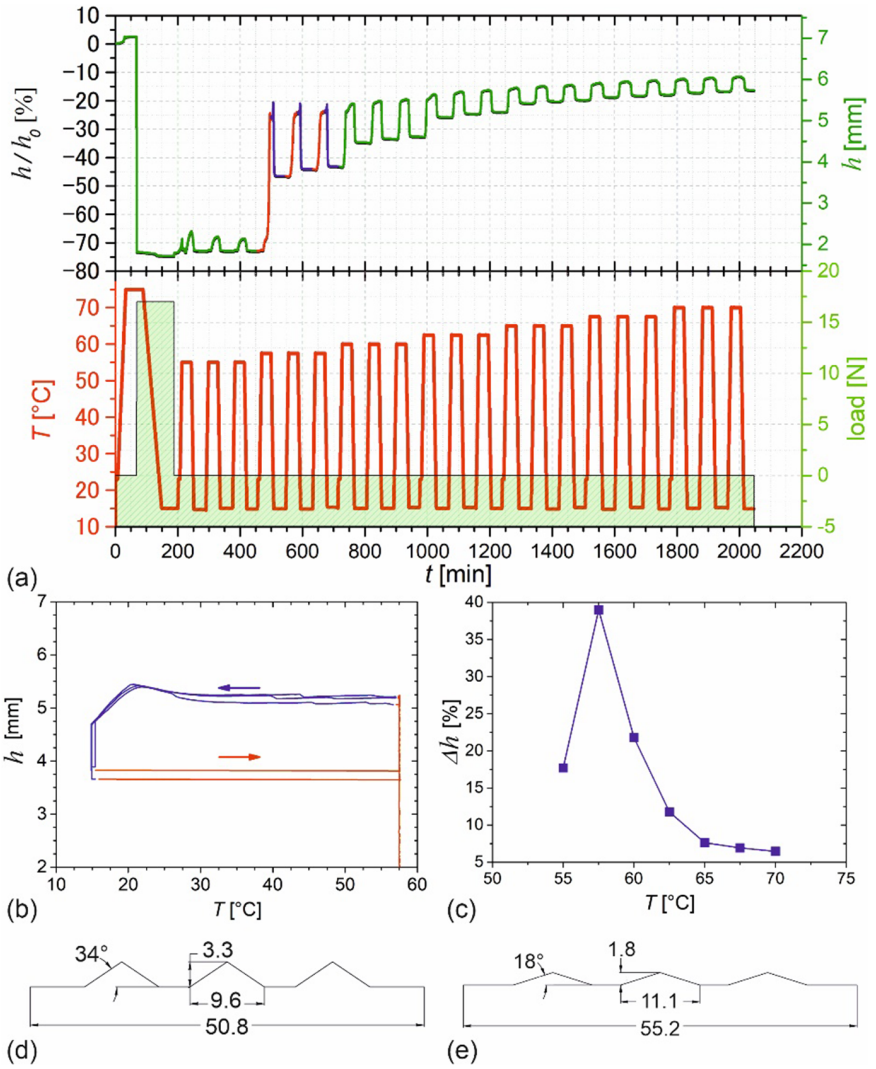

Figure 3. *Influence of the selection of T_{max} on the actuation of a programmable gear made from a PDA-based PEU. After thermomechanical treatment, a weak external load of 0.01 N was applied: Evolution of (a) changes in object height h/h_0, sample height h (red and blue colour for heating and cooling, respectively) and temperature T (bottom graph) over measurement time t, (b) evolution of object height h upon temperature cycling between 15°C and 58°C, and (c) Δh depending on T_{max} (all values are averaged for the second and third thermal cycles). The corresponding states of the gear in (d) its first temperature bistable state characterised by a small outer diameter at T_{max} = 58°C, and (e) its second temperature bistable and mostly expanded state, characterised by a maximum outer diameter at T_{low} = 15°C. In panels (d,e), the dimensions are provided in millimetres.*

15°C are illustrated in Figure 3d,e. They suggest that during actuation, a change in height of 1.5 mm was accompanied by a change in diameter of 4.4 mm. The further increase of T_{max} above 58°C gave a decrease in actuation due to the systematic melting of PDA crystals as witnessed in the DSC measurement (Figure 1a), which resulted in the steady recovery of the original shape and thus a lower overall change in h/h_0. In other words, the elongation at the beginning of each cooling step was gradually shifted to higher values and recovered large parts of the initial shape of the object. Obviously,

https://doi.org/10.1017/pma.2023.9 Published online by Cambridge University Press

under these conditions, oriented PDA crystals serving as physical netpoints were molten and no longer available to support the structural integrity associated with the respective temperature bistable states of the polymer. The observed decrease in actuation with increasing cycle number is a phenomenon that has already been witnessed many times before (Behl et al., 2013; Bothe et al., 2013; Zhou et al., 2014; Fan et al., 2018a,b).

However, for the material investigated here, it could already be shown that the actuation stabilises in a temperature regime between 15°C and 64°C after about 25 heating–cooling cycles (Schönfeld et al., 2021). One way to estimate thermal actuation is to carry out a temperature conditioning at the higher actuation temperature (T_{max}). In this context, it was demonstrated for the PEU that after deformation and a temperature holding time of 70 hr at 62°C, the length of the sample can be estimated in one of its temperature bistable states (Schönfeld et al., 2021). Repeated stretching and relaxation at the higher actuation temperature may be an option to ensure that entanglements within the polymer are broken, allowing equilibrium states to be established more quickly.

When investigating the actuation of the PEU, it is important to keep in mind that an exceeding of the upper switching temperature can erase the 2W-SME. In fact, heating to 75°C resulted in a complete recovery to the original shape (Figure 2h), so that thermal bistability was lost. In this context, it will be important in the future to have a precise understanding of the maximum possible temperature under conditions relevant to the application.

Conceptually, the object can be used wherever the change in shape can assure or interrupt the transmission of a force and thus, for example, prevent systems from overheating. An even more precise on/off switch may be realised by introducing programmable materials with structurally bistable states when selecting unit cells containing bridges, which force the material to gain either a first or a second shape (Berwind et al., 2018). In this case, the transformation between the two radii of such a gear would enable the material to switch to ‘go’ so that a clear coupling/decoupling can be achieved.

In a progressive approach a thermally switchable ‘bevel gearbox’ was developed (Figure 4).

The ‘bevel gearbox’ was composed of a standard bevel gear as input gear (Figure 4a,b) and an assembled actuating ‘gear’ as output gear (Figure 4c–e). The standard bevel gear was characterised by an outer diameter of 66.7 mm (Figure 4a). It was additively manufactured via FFF (Figure 4b). For the actuating gear, the individual teeth were first designed (Figure 4c), then additively manufactured by means of FFF (Figure 4d, left) and thermomechanically treated, whereupon they took a straight shape (Figure 4d, right). Later, the 12 ‘teeth’ were mounted on a gear base cut out from a 5 mm thick poly(methyl methacrylate) sheet (Figure 4e). Here, a spring-loaded disc was placed on the top of the base plate, which ensured that the actuating teeth did not completely regain their initial shape if the upper temperature was exceeded. The spring-loaded disc and the teeth were 7 mm apart at 23°C, so that the teeth were in a stress-free state. Finally, the input and output bevel gears were assembled to form a gearbox, whereupon the system was ready to use (Figure 4e). From a design perspective, full gearing was selected to ensure better safety and to allow quick re-engagement of the force at any tooth position during rotation. For functional proof-of-principle, the input gear was set in motion and the temperature was cycled three times between 23°C and 58°C (Figure 5, S1.movie in Supplementary Material).

At 23°C, the input gear and the output gear were in contact, permitting a power transmission (Figure 5). Upon raising the temperature to 58°C, the ‘teeth’ recovered their high-temperature stable shape, which disengaged the power transmission. Later on, cooling to 23°C resulted in the return of the ‘teeth’ into their low-temperature stable shape, which was accompanied by re-engaging the power transmission.

To ensure that programming can also be used to obtain temperature bistable states in other programmable materials and thus to verify distinct actuation with regard to changes in the length of a sample, a unit cell was designed (Figure 6a–d). Additionally, a simulation was conducted to understand the sample behaviour during compressive deformation in course of thermomechanical treatment (Figure 6e,f).

The unit cell was conceptualised in such a way that the two opposite beams protruded slightly in the middle (Figure 6a–d). When the upper and lower parts of the unit cell were pressed together, the beams

https://doi.org/10.1017/pma.2023.9 Published online by Cambridge University Press

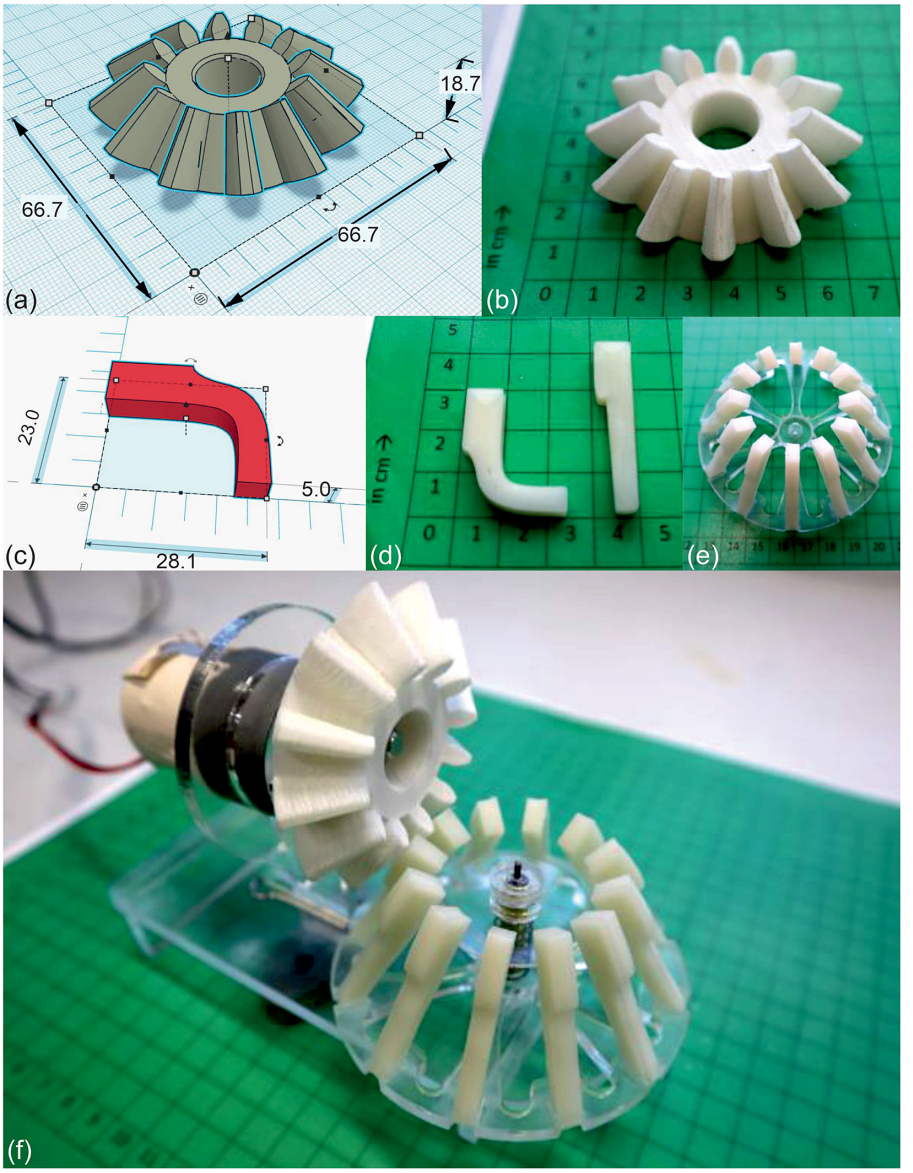

Figure 4. *Thermally switchable 'bevel gearbox': (a) A technical drawing of the input bevel gear and (b) the additively manufactured 'output bevel gear'. (c) A technical drawing of one of the 'teeth' of the 'bevel gear', (d, left) an additively manufactured 'tooth', (d, right) a 'tooth' after thermomechanical treatment to implement thermoresponsiveness, and (e) the assembled output 'bevel gear' containing 12 thermoresponsive 'teeth'. (f) Gearbox consisting of the input bevel gear and the assembled 'output bevel gear'. In panels (a,c), the dimensions are provided in millimetres.*

pulled outward and reached the maximum bending for each beam segment, as shown in the simulation (Figure 6e,f). It can be clearly seen that the maximum von Mises stresses occurred at the middle part of the unit cell, where the beams protruded.

After three-dimensional (3D) printing, the unit cell (Figure 7a) was found to have an excellent dimensional accuracy when compared to the computer aided design (CAD) model (Figure 6a). Once programmed (Figure 7b), the new shape was stable at 23°C and showed an overall length l of 23.8 mm.

https://doi.org/10.1017/pma.2023.9 Published online by Cambridge University Press

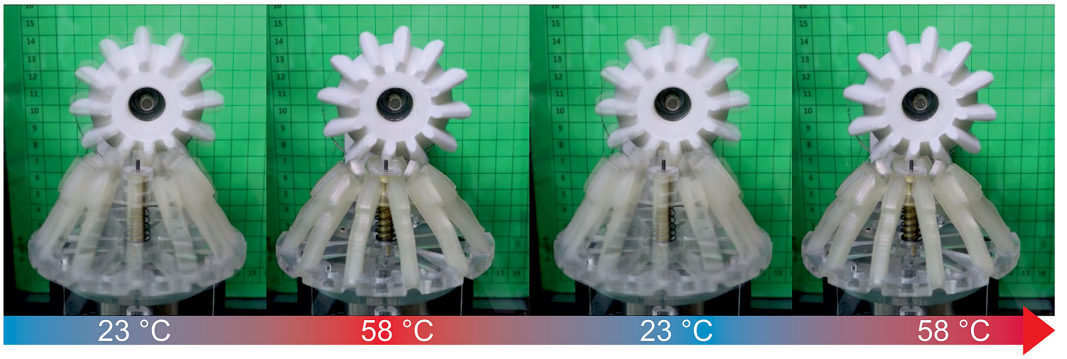

Figure 5. *A thermally switchable 'bevel gearbox'. The actuating gear switches the power transmission on at about 23°C and off at approximately 58°C.*

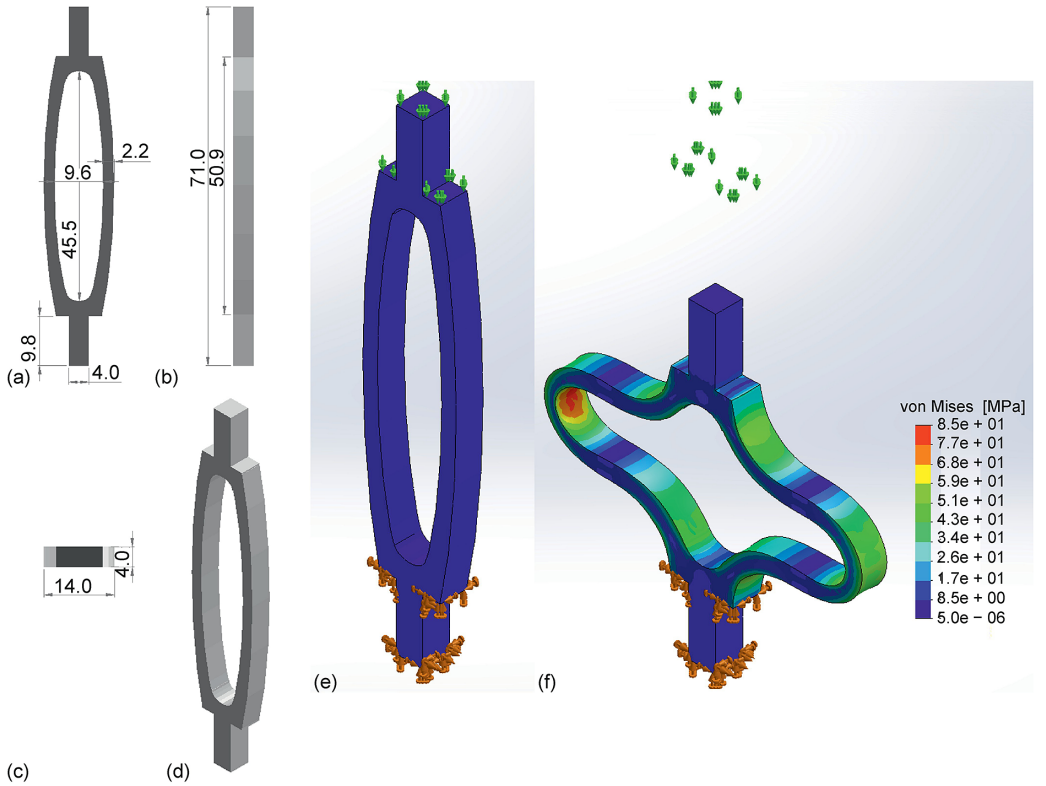

Figure 6. *Technical drawing of a unit cell in the perspectives (a) front view, (b) right view, (c) top view, and (d) isometric view. The von Mises stress distribution (e) before and (f) after deformation. In panels (a–c), the dimensions are provided in millimetres.*

Subsequently, the 2W-SME was examined. On raising the temperature to 58°C, the unit cell attained its second bistable state by expanding into the opposite direction of deformation. The resulting shape was characterised by a length of 35.6 mm (Figure 7c). Thus, a change in length Δl of about 50% could be witnessed. Once cooled back to 23°C, the initial bistable state of the unit cell was reached by contraction in the direction of deformation (Figure 7d). This resulted in a decrease in length to 24.6 mm, corresponding to a change in Δl of about 45%. The actuation was proven by another cycle of heating

https://doi.org/10.1017/pma.2023.9 Published online by Cambridge University Press

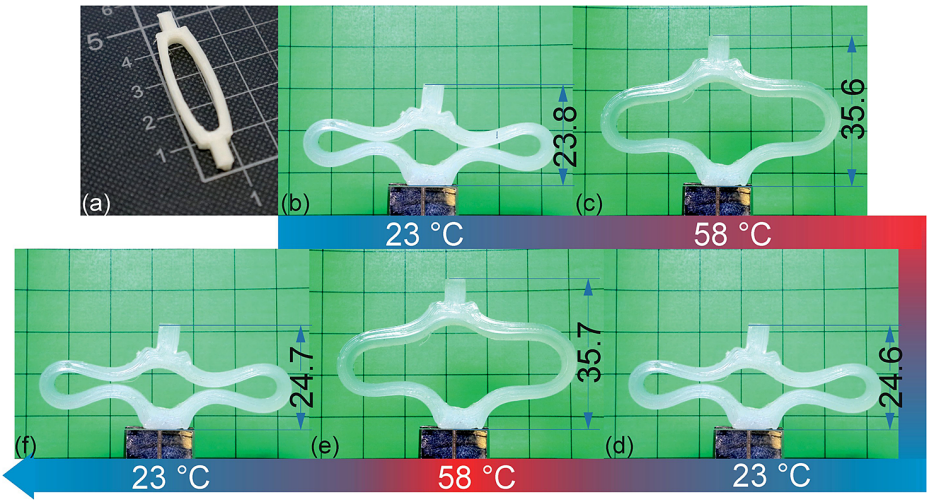

Figure 7. *Unit cell made from PDA-based PEU in its (a) permanent shape as obtained after fused filament fabrication, (b) programmed shape, and (c–f) shapes during switching between the temperature bistable states. In the background, centimetre paper is exhibited (all the dimensions are given in mm).*

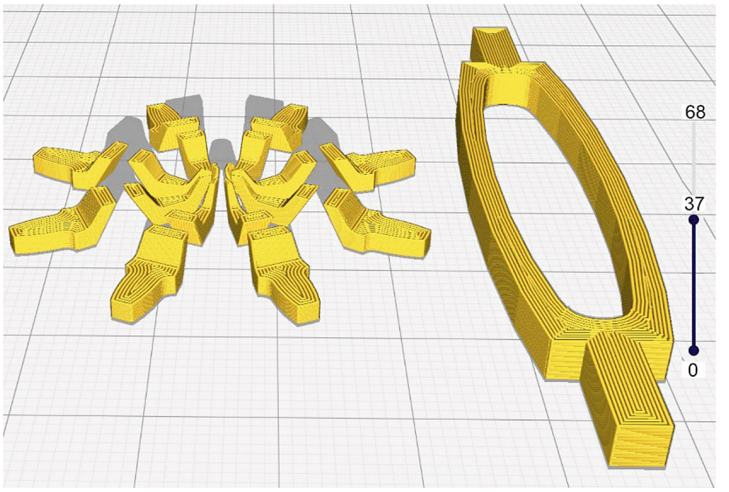

Figure 8. *Strand deposition orientation as obtained with Cura slicer software for (left) the gear-like object and (right) the unit cell.*

and cooling (Figure 7e,f) and by two further ones (S2.movie in Supplementary Material). Interestingly, the thermal expansion coefficient of an untreated PEU sample between 23°C and 58°C was quantified in a DMA measurement to be about $3.23 \times 10^{-5}\,°C^{-1}$ (see Supplementary Figure S1). In so far, thermal expansion made only a small contribution to the proven actuation during heating. Instead, it was the programmed material behaviour that determined the actuation. Apart of differences in the overall shape of the demonstrators, their programming and internal stress distribution, the slightly higher actuation of the unit cell compared to the gear-like object (Figure 2h) is supposed to be also supported by strand orientation during printing (Figure 8).

Indeed, compared to the gear-like object (Figure 2h), the unit cell exhibited a higher proportion of polymer strands arranged parallel to each other and, at the same time, roughly in the direction of force

https://doi.org/10.1017/pma.2023.9 Published online by Cambridge University Press

application in the course of deformation during programming. This also suggests a higher degree of order in the unit cell once it had assumed one of the temperature bistable states. However, detailed studies on stress distribution in thermally actuating objects are needed to gain a better understanding of material behaviour.

In summary, the paths taken here lead to significantly higher actuation compared to solid materials, as the programmable materials approach combines the functionality of external structure with the molecular design. More specifically, in one of our previous works, the same PEU as a solid material showed only a maximum thermal actuation of about 16% after programming in which the deformation was introduced by stretching (Schönfeld et al., 2021). In perspective, significant actuation may assist in opening the door to new applications, for example, in the field of robotics. Reducing the size of the unit cell can help to lower the complexity in previously presented actuating systems. For example, a PEU actuator as functional component of a gripper, as presented in one of our previous works (Schönfeld et al., 2021), could be produced from smaller programmable materials. Ideally, this also allows material to be saved, so that such approaches can make a contribution to sustainability.

Conclusions

This work unveils that thermoresponsive programmable materials made of PEU are capable of both drastic and complex shape changes, which cannot be witnessed when using classical design approaches for 2W SMPs. This way, the melting and crystallisation of the PEU's soft segment allowed a force transmission to be activated and deactivated by changing the ambient temperature of a 'bevel gear', equipped with 2W actuating elements. Such approaches could, for instance, reduce the complexity and size of grippers. In terms of the design of future thermoresponsive programmable materials, the following strategies would be worth considering:

1. The synthesis of PEUs with high-temperature stable switching segments may allow that the 2W-SME cannot be extinguished under clearly defined application conditions.
2. Deformation-induced crystallisation during programming may result in thermal actuators, whose soft segment melting temperature stability will be enhanced, when the deformation temperature exceeds the offset melting transition temperature of the switching segment. Here, it is particularly important to find out how great the improvement in thermal stability can be.
3. Particularly strong orientations of the polymer chains such as may be introduced by additive manufacturing processes could contribute to higher actuation capability. In this context, further potential should soon arise from activities in the field of 4D printing.
4. Approaches like blending of PEUs with distinct actuation could combine the advantageous properties of both partners in one programmable material.
5. The combination of different types of programmable materials could be a key to enable more complex switching processes, which could be supported by modifications in the design of the unit cells and their application-specific programming.
6. Unit cells may be equipped with wires for heating purposes. This could be done by adapting the printing process, as it creates possibilities for local heating of polymers including complex motion and, in addition, control over mechanical properties.

All of this illustrates that there are multiple opportunities to tailor the properties of thermoresponsive programmable materials for specific applications, further expanding existing capabilities.

Experimental section

Material

The same PDA-based PEU, which was synthesised recently (Schönfeld et al., 2021), was selected as the base material for this work. The material was used in the form of filament for 3D printing.

https://doi.org/10.1017/pma.2023.9 Published online by Cambridge University Press

Table 1. *Printing parameters selected for additive manufacturing.*

Printing parameters	PEU
Diameter of the nozzle (μm)	400
Temperature of the nozzle (°C)	208
Speed of print head (mm·s^{-1})	15
Build platform temperature (°C)	75
Layer height (mm)	0.1

Abbreviation: PEU, polyester urethane.

Virtual design and fused filament fabrication

The AutoCAD software from Autodesk, Inc., (San Rafael, CA, USA) was employed to design programmable materials in the form of a 'gear' and 2W-actuating teeth of a bevel gear. The programmable material in the form of a unit cell was designed and simulated by means of Solidworks from Dassault Systèmes (Vélizy-Villacoublay, Île-de-France, France). The developed CAD models were exported as standard triangle language (STL) files and later used for slicing. After finalising the design of the gears and of the unit cell, Cura 3.6.1 (Ultimaker, 2023) was used as a slicer program to generate numerically controlled codes, also denoted as G-codes. The 3D models were imported into the program and sliced into layers according to the predefined printing parameters (Table 1). The most relevant settings for additive manufacturing (AM) are listed in Table 1. To start AM, the generated G-codes were transferred to the 3D printer. The 3D printed objects were produced by FFF using the commercially available 3D printer Ultimaker 3 from Ultimaker B.V. (Utrecht, The Netherlands).

Characterisation of thermal properties

The phase transition behaviour of PDA-based PEU was characterised by DSC using a Q100 DSC from TA Instruments (New Castle, DE, USA). The measurements were conducted on the centre part of an additively manufactured type 5B tensile bar according to ISO 527-2:1996. The sample had a weight of 5 mg.

The PEU was thermally cycled between −50°C and 225°C. For cooling and heating, a rate of 10°C min^{-1} was applied. The temperature holding time at the minimum and maximum temperatures was 2 min.

Characterisation of thermomechanical properties

The thermomechanical properties of the PEU were studied by DMA. The experiments were carried out with a Q800 DMA from TA Instruments (New Castle, DE, USA) using film tension clamps on multi-frequency-strain mode. A frequency of 10 Hz, a static force of 0.1 N and an oscillating amplitude of 10 μm were selected to investigate the centre part of an additively manufactured type 5B tensile bar according to ISO 527-2:1996. At first, the sample was cooled to −80°C and held there for 5 min, before it was heated to 100°C with a rate of 3°C min^{-1}. In parallel, the evolution in storage modulus E' and loss factor tan δ was determined.

Programming and characterisation of 2W-SME

The programmable materials made from PDA-based PEU were both thermomechanically treated (programmed) and the actuation was analysed with a Q800 DMA from TA Instruments (New Castle, DE, USA). In order to characterise the 2W-SME, the gear-like object was initially placed between two compression clamps. The chamber was heated to 75°C at the beginning of thermomechanical treatment. After holding the temperature at 75°C constant for 30 min, the object was compressed with

https://doi.org/10.1017/pma.2023.9 Published online by Cambridge University Press

a force of 17 N using a loading rate of 1 N·min^{-1}. Then, the deformed object was cooled to 15°C while maintaining the compressive force. The temperature T_{min} was maintained for 30 min. Subsequently, the applied force was unloaded with a rate of 1 N·min^{-1}, and the object was heated to 23°C and held at that temperature for another 5 min to mark the end of programming. The actuation of the programmable material was studied under a constant external load of 0.01 N by cycling the temperature. In detail, the sample was heated from 23°C to T_{max} = 55°C and held there for 30 min, before it was cooled to T_{min} = 15°C, at which the temperature was kept for another 30 min. Heating and cooling were carried out three times. Afterward, T_{max} was increased from 55°C to 70°C with an increment of 2.5°C, and for each increment, the temperature was cycled between T_{min} and T_{max} for three times. Heating and cooling rates of 5°C·min^{-1} were used for the whole experiment. In case of the bevel gear, the 'teeth' were also made from PEU. Twelve teeth in their original bent shape were placed in a programming template, heated to 75°C in a UF110 heating chamber from Memmert GmbH + Co. KG (Schwabach, Germany) and deformed at the same time in order to gain the teeth in a straight state, compare Figure 4d (right). Once cooled to 15°C and unloaded, the teeth were mounted on a gear base along with a spring-loaded disc cut out of a 5 mm thick poly(methyl methacrylate) sheet with a clearance of about 7 mm, so that they were in a stress-free state at 23°C. Later, the input and the output 'bevel gear' were assembled in a gearbox. For functional characterisation, the setup was placed in the environmental chamber of an MTS Criterion universal testing machine (model 43) from MTS Systems Corporation (Eden Prairie, MN, USA) equipped with a liquid nitrogen Dewar vessel. The actuation was then characterised by temperature changes between 58°C (T_{max}) and 23°C (T_{min}) in three cycles. In case of the unit cell, the thermomechanical treatment was conducted with an MTS Criterion universal testing machine (model 43) from MTS Systems Corporation (Eden Prairie, MN, USA). The device was equipped with a 500 N load cell and was operated with a temperature chamber, which was controlled by a Eurotherm temperature controller unit. Two heating elements were located at the back of the chamber. Liquid nitrogen from a Dewar's vessel was fed into the chamber under a pressure of 1.3 bar as an essential prerequisite for cooling. At the beginning of thermomechanical treatment, the thermochamber was preheated to 75°C, and the unit cell was fixed in the pneumatic clamps of the universal testing machine using a clamping air pressure of 0.4 bar. After 30 min at 75°C, the unit cell was compressed in such a way that the top part touched the bottom using a loading rate of 1 N·min^{-1}. In the next step, the temperature was brought to 15°C and held there for 30 min to fix the new shape while maintaining the compressive load. Then, the unit cell was unloaded with a rate of 1 N·min^{-1}. The temperature was then heated to 23°C, and the unit cell was removed from the clamps.

The 2W-SME of the programmable material was subsequently characterised by unclamping only from the upper clamp and cycling the temperature between 58°C (T_{max}) and 23°C (T_{min}).

The thermoreversible changes in height Δh and length Δl of the studied samples were quantified according to equations (1) and (2):

$$\Delta h = \left(\frac{h_{Tmax}(N)}{h_{Tmin}(N)} - 1 \right) \cdot 100\%, \tag{1}$$

$$\Delta l = \left(\frac{l_{Tmax}(N)}{l_{Tmin}(N)} - 1 \right) \cdot 100\%. \tag{2}$$

Herein, $h_{Tmin}(N)$ and $h_{Tmax}(N)$ are the heights of a programmable material in the Nth cycle of actuation at T_{min} and T_{max}. Accordingly, $l_{Tmin}(N)$ and $l_{Tmax}(N)$ are the lengths of the programmable material in the Nth cycle of actuation at T_{min} and T_{max}.

Thermal expansion coefficient

The thermal expansion coefficient α of the PEU was determined with a Q800 DMA from TA Instruments (New Castle, DE, USA). The untreated sample in the form of a tensile bar of type 5B according to ISO 527-2:1996 was fixed in a film clamp. The temperature was raised from 23°C to

https://doi.org/10.1017/pma.2023.9 Published online by Cambridge University Press

75°C and the expansion behaviour followed. Later, the sample was cooled to 23°C and heated to 58°C, before the temperature was cycled between 58°C and 23°C for four times. At 23°C, 58°C, and 75°C, the temperatures were held for 15 min, and a heating and cooling rate of 5°C mm^{-1} was chosen throughout the experiment. The length of the sample at the end of holding time at 23°C and 58°C was used to determine the thermal expansion coefficient of the PEU according to equation (3)), and the mean value was determined for cycles one to five.

$$\alpha = \frac{\Delta l}{l_0 \bullet \Delta T}. \tag{3}$$

Here, Δl defines the change in the length of the sample, l_0 is its initial length, and ΔT the temperature difference between 58°C and 23°C, which is here of 35°C.

Simulation

The simulation of the programmable material with regard to the unit cell was conducted using Solidworks from Dassault Systèmes (Vélizy-Villacoublay, Île-de-France, France). After CAD modelling, the simulation was carried out in a nonlinear-static study, where the bottom part of the sample (orange arrows in Figure 6e,f) was fixed while a pressure of 10 $N{\cdot}mm^{-2}$ was applied on its top part (green arrows in Figure 6e,f). After simulation, the von Mises stresses were analysed.

Supplementary material. The supplementary material for this article can be found at http://doi.org/10.1017/pma.2023.9. Supplementary videos: S1.movie: Thermally switchable 'bevel gearbox' (Figure 5) and S2.movie: Actuating unit cell (Figure 7).

Acknowledgements. The working group of Fraunhofer IAP wishes to thank the European Regional Development Fund for financing a large part of the laboratory equipment (project 85007031) and the Fraunhofer High-Performance Center 'Integration of Biological and Physical–Chemical Material Functions' in Potsdam-Golm for the funding of some of the FFF printers (project 630505). Dr. Mario Walter and Dennis Schönfeld are acknowledged for carrying out polymer synthesis.

Funding statement. This work was carried out in two projects within the Fraunhofer Cluster of Excellence 'Programmable Materials' (PSP elements 40-04068-2500-00007 and 40-01922-2500-00003).

Competing interest. The authors declare no competing interests exist.

References

Behl M, **Kratz K**, **Zotzmann J**, **Nöchel U** and **Lendlein A** (2013b) Reversible bidirectional shape-memory polymers. *Advanced Materials* **25**, 4466–4469. https://doi.org/1002/adma.201300880

Behl M, **Kratz K**, **Noechel U**, **Sauter T** and **Lendlein A** (2013a) Temperature-memory polymer actuators. *PNAS* **110**, 12555–12559. https://doi.org/1073/pnas.1301895110

Berwind MF, **Kamas A** and **Eberl C** (2018) A hierarchical programmable mechanical metamaterial unit cell showing metastable shape memory. *Advanced Engineering Materials* **20**, 1800771. https://doi.org/1002/adem.201800771

Bothe M and **Pretsch T** (2012) Two-way shape changes of a shape-memory poly(ester urethane). *Macromolecular Chemistry and Physics* **213**, 2378–2385. https://doi.org/1002/macp.201200096

Bothe M, **Emmerling F** and **Pretsch T** (2013) Poly(ester urethane) with varying polyester chain length: Polymorphism and shape-memory behavior. *Macromolecular Chemistry and Physics* **214**, 2683–2693. https://doi.org/1002/macp.201300464

Chalissery D, **Pretsch T**, **Staub S** and **Andrä H** (2019) Additive manufacturing of information carriers based on shape memory polyester urethane. *Polymers* **2019**, 11. https://doi.org/3390/polym11061005

Chalissery D, **Schönfeld D**, **Walter M**, **Ziervogel F** and **Pretsch T** (2022) Fused filament fabrication of actuating objects. *Macromolecular Materials and Engineering* **307**, 2200214. https://doi.org/1002/mame.202200214

Chalissery D (2023) Fused filament fabrication to manufacture three- and four-dimensional objects made of shape memory polymers. Doctoral thesis. Berlin: Technische Universität Berlin. https://doi.org/14279/depositonce-17051

Chung T, **Romo-Uribe A** and **Mather PT** (2008) Two-way reversible shape memory in a Semicrystalline network. *Macromolecules* **41**, 184–192. https://doi.org/1021/ma071517z

Dietsch B and **Tong T** (2007) A review features and benefits of shape memory polymers (smps). *Journal of Advanced Materials* **39**, 3–12.

Fan LF, **Rong MZ**, **Zhang MQ** and **Chen XD** (2017) A facile approach toward scalable fabrication of reversible shape-memory polymers with bonded elastomer microphases as internal stress provider. *Macromolecular Rapid Communications* **38**, 1700124. https://doi.org/1002/marc.201700124

Fan LF, **Rong MZ**, **Zhang MQ** and **Chen XD** (2018a) A very simple strategy for preparing external stress-free two-way shape memory polymers by making use of hydrogen bonds. *Macromolecular Rapid Communications* **39**, e1700714. https://doi.org/1002/marc.201700714

Fan LF, **Rong MZ**, **Zhang MQ** and **Chen XD** (2018b) Dynamic reversible bonds enable external stress-free two-way shape memory effect of a polymer network and the interrelated intrinsic self-healability of wider crack and recyclability. *Journal of Materials Chemistry A* **6**, 16053–16063. https://doi.org/1039/C8TA05751F

Fan LF, **Huang YN**, **Rong MZ** and **Zhang MQ** (2020) A simple and universal strategy for preparing external stress-free two-way shape memory polymers by making use of the chemical crosslinkages derived from peroxide initiator. *Express Polymer Letters* **14**, 295–308. https://doi.org/3144/expresspolymlett.2020.26

Fischer SCL, **Hillen L** and **Eberl C** (2020) Mechanical metamaterials on the way from laboratory scale to industrial applications:Challenges for characterization and scalability. *Materials (Basel)* **13**, 3605. https://doi.org/3390/ma13163605

Hager MD, **Bode S Weber C** and **Schubert US** (2015) Shape memory polymers: Past, present and future developments. *Progress in Polymer Science* **49–50**, 3–33. https://doi.org/1016/j.progpolymsci.2015.04.002

Hoffman AS (2013) Stimuli-responsive polymers: Biomedical applications and challenges for clinical translation. *Advanced Drug Delivery Reviews* **65**, 10–16. https://doi.org/1016/j.addr.2012.11.004

Holme (1806) VII a description of a property of caoutchouc, or indian rubber; with some reflections on the cause of the elasticity of this substance. In a letter to Dr.Holme. *The Philosophical Magazine* **24**, 39–43. https://doi.org/1080/14786440608563329

Huang WM, **Yang B**, **Zhao Y** and **Ding Z** (2010) Thermo-moisture responsive polyurethane shape-memory polymer and composites: A review. *Journal of Materials Chemistry* **20**, 3367. https://doi.org/1039/b922943d

Ji FL, **Hu JL**, **Li TC** and **Wong YW** (2007) Morphology and shape memory effect of segmented polyurethanes. Part I: With crystalline reversible phase. *Polymer* **48**, 5133–5145. https://doi.org/1016/j.polymer.2007.06.032

Jin L, **Forte AE**, **Deng B**, **Rafsanjani A** and **Bertoldi K** (2020) Kirigami-inspired inflatables with programmable shapes. *Advanced Materials* **32**, e2001863. https://doi.org/1002/adma.202001863

Ke D, **Chen Z**, **Momo ZY**, **Jiani W**, **Xuan C**, **Xiaojie Y** and **Xueliang X** (2020) Recent advances of two-way shape memory polymers and four-dimensional printing under stress-free conditions. *Smart Materials and Structures* **29**, 23001. https://doi.org/1088/1361-665X/ab5e6d

Kim BK, **Lee SY** and **Xu M** (1996) Polyurethanes having shape memory effects. *Polymer* **37**, 5781–5793. https://doi.org/1016/S0032-3861(96)00442-9

Kim Y-J and **Matsunaga YT** (2017) Thermo-responsive polymers and their application as smart biomaterials. *Journal of Materials Chemistry B* **5**, 4307–4321. https://doi.org/1039/c7tb00157f

Lee BS, **Chun BC**, **Chung Y-C**, **Sul KI** and **Cho JW** (2001) Structure and thermomechanical properties of polyurethane block copolymers with shape memory effect. *Macromolecules* **34**, 6431–6437. https://doi.org/1021/ma0018421

Li F, **Zhang X**, **Hou J**, **Xu M**, **Luo X**, **Ma D** and **Kim BK** (1997) Studies on thermally stimulated shape memory effect of segmented polyurethanes. *Journal of Applied Polymer Science* **64**, 1511–1516. https://doi.org/1002/(SICI)1097-4628(19970523)64:8<1511:AIDAPP8>3.0.CO;2-K

Liu C, **Qin H** and **Mather PT** (2007) Review of progress in shape-memory polymers . *Journal of Materials Chemistry* **17**, 1543. https://doi.org/1039/b615954k

Liu W, **Zhang R**, **Huang M**, **Dong X**, **Xu W**, **Wang Y**, **Hu G-H** and **Zhu J** (2016) Synthesis and shape memory property of segmented poly(ester urethane) with poly(butylene 1,4-cyclohexanedicarboxylate) as the soft segment. *RSC Advances* **6**, 95527–95534. https://doi.org/1039/C6RA16325D

Mirtschin N and **Pretsch T** (2017) Programming of one- and two-step stress recovery in a poly(ester urethane). *Polymers* **9**, 98. https://doi.org/3390/polym9030098

Müller WW and **Pretsch T** (2010) Hydrolytic aging of crystallizable shape memory poly(ester urethane): Effects on the thermo-mechanical properties and visco-elastic modeling. *European Polymer Journal* **46**, 1745–1758. https://doi.org/1016/j.eurpolymj.2010.05.004

Pereira IM and **Oréfice RL** (2010) The morphology and phase mixing studies on poly(ester-urethane) during shape memory cycle. *Journal of Materials Science* **45**, 511–522. https://doi.org/1007/s10853-009-3969-7

Petchsuk A, **Klinsukhon W**, **Sirikittikul D** and **Prahsarn C** (2012) Parameters affecting transition temperatures of poly(lactic acid-copolydiols) copolymer-based polyester urethanes and their shape memory behavior. *Polymers for Advanced Technologies* **23**, 1166–1173. https://doi.org/1002/pat.2017

Pretsch T (2010) Review on the functional determinants and durability of shape memory polymers. *Polymers* **2**, 120–158. https://doi.org/3390/polym2030120

Pretsch T and **Müller WW** (2010) Shape memory poly(ester urethane) with improved hydrolytic stability. *Polymer Degradation and Stability* **95**, 880–888. https://doi.org/1016/j.polymdegradstab.2009.12.020

Ratna D and **Karger-Kocsis J** (2008) Recent advances in shape memory polymers and composites: A review. *Journal of Materials Science* **43**, 254–269. https://doi.org/1007/s10853-007-2176-7

Ren H, **Mei Z**, **Chen S**, **Zhuo H**, **Chen S**, **Yang H**, **Zuo J** and **Ge Z** (2016) A new strategy for designing multi-functional shape memory polymers with amine-containing polyurethanes. *Journal of Materials Science* **51**, 9131–9144. https://doi.org/1007/s10853-016-0166-3

Restrepo D, **Mankame ND** and **Zavattieri PD** (2016) Programmable materials based on periodic cellular solids. Part I: Experiments. *International Journal of Solids and Structures* **100**–101, 485–504. https://doi.org/1016/j.ijsolstr.2016.09.021

https://doi.org/10.1017/pma.2023.9 Published online by Cambridge University Press

Scalet G (2020) Two-way and multiple-way shape memory polymers for soft robotics: An overview. *Actuators* **9**, 10. https://doi.org/3390/act9010010

Schönfeld D, **Chalissery D**, **Wenz F**, **Specht M**, **Eberl C** and **Pretsch T** (2021) Actuating shape memory polymer for thermoresponsive soft robotic gripper and programmable materials. *Molecules* **26**, 522. https://doi.org/3390/molecules26030522

Specht M, **Berwind M** and **Eberl C** (2021) Adaptive wettability of a programmable metasurface. *Advanced Engineering Materials* **23**, 2001037. https://doi.org/1002/adem.202001037

Sun L, **Huang WM**, **Ding Z**, **Zhao Y**, **Wang CC**, **Purnawali H** and **Tang C** (2012) Stimulus-responsive shape memory materials a review. *Materials & Design* **33**, 577–640. https://doi.org/1016/j.matdes.2011.04.065

Takeuchi N, **Nakajima S**, **Yoshida K**, **Kawano R**, **Hori Y** and **Onoe H** (2022) Microfiber-shaped programmable materials with stimuli-responsive hydrogel. *Soft Robotics* **9**, 89–97. https://doi.org/1089/soro.2020.0038

Ultimaker Cura (2023) Ultimaker Cura: Powerful, Easy-to-Use 3D Printing Software. Available online: https://ultimaker.com/software/ultimaker-cura (accessed on 15 March 2023).

Walter M, **Friess F**, **Krus M**, **Zolanvari SMH**, **Grün G**, **Kröber H** and **Pretsch T** (2020) Shape memory polymer foam with programmable apertures. *Polymers* **12**, 1914. https://doi.org/3390/polym12091914

Wang W, **Jin Y**, **Ping P**, **Chen X**, **Jing X** and **Su Z** (2010) Structure evolution in segmented poly(ester urethane) in shape-memory process. *Macromolecules* **43**, 2942–2947. https://doi.org/1021/ma902781e

Westbrook KK, **Mather PT**, **Parakh V**, **Dunn ML**, **Ge Q**, **Lee BM** and **Qi HJ** (2011) Two-way reversible shape memory effects in a free-standing polymer composite. *Smart Materials and Structures* **20**, 65010. https://doi.org/1088/0964-1726/20/6/065010

Yin X, **Hoffman AS** and **Stayton PS** (2006) Poly(N-isopropylacrylamide-co-propylacrylic acid) copolymers that respond sharply to temperature and pH. *Biomacromolecules* **7**, 1381–1385. https://doi.org/1021/bm0507812

Zare M, **Prabhakaran MP**, **Parvin N** and **Ramakrishna S** (2019) Thermally-induced two-way shape memory polymers: Mechanisms, structures, and applications. *Chemical Engineering Journal* **374**, 706–720. https://doi.org/1016/j.cej.2019.05.167

Zhang X, **Pint CL**, **Lee MH**, **Schubert BE**, **Jamshidi A**, **Takei K**, **Ko H**, **Gillies A**, **Bardhan R**, **Urban JJ**, **Wu M**, **Fearing R** and **Javey A** (2011) Optically- and thermally-responsive programmable materials based on carbon nanotube-hydrogel polymer composites. *Nano Letters* **11**, 3239–3244. https://doi.org/1021/nl201503e

Zhao Q, **Qi HJ** and **Xie T** (2015) Recent progress in shape memory polymer: New behavior, enabling materials, and mechanistic understanding. *Progress in Polymer Science* **49**–50, 79–120. https://doi.org/1016/j.progpolymsci.2015.04.001

Zhou J, **Turner SA**, **Brosnan SM**, **Li Q**, **Carrillo J-MY**, **Nykypanchuk D**, **Gang O**, **Ashby VS**, **Dobrynin AV** and **Sheiko SS** (2014) Shapeshifting: Reversible shape memory in Semicrystalline elastomers. *Macromolecules* **47**, 1768–1776. https://doi.org/1021/ma4023185

Cite this article: Chalissery, D., Rümmler, T., Ziervogel, F., Eberl, C., and Pretsch, T. (2023). Harnessing length and height changes in thermoresponsive programmable materials. *Programmable Materials*, **1**, e10. https://doi.org/10.1017/pma.2023.9